Kintanar, A., Huang, W.-C., Schindele, D. C., Wemmer, D. E., & Drobny, G. (1989) *Biochemistry 28*, 282-293.
Kopka, M. L., Frantini, A. V., Drew, H. R., & Dickerson, R. E. (1983) *J. Mol. Biol. 163*, 129-146.
Luz, Z., Poupko, R., & Samulski, E. T. (1981) *J. Chem. Phys. 74*, 5825-5837.
Nall, B. T., Rothwell, W. P., Waugh, J. S., & Rupprecht, A. (1981) *Biochemistry 20*, 1881-1887.
Nerdal, W., Hare, D. R., & Reid, B. R. (1989) *Biochemistry 28*, 10008-10021.
Nicholson, L. K., Moll, F., Mixon, T. E., LoGrasso, P. V., Lay, J. C., & Cross, T. A. (1987) *Biochemistry 26*, 6621-6626.
Privé, G. G., Heinemann, U., Chandrasegaran, S., Kan, L.-S., Kopka, M. L., & Dickerson, R. E. (1987) *Science 238*, 498-503.
Reid, B. R. (1987) *Q. Rev. Biophys. 20*, 1-34.
Rill, R. L. (1986) *Proc. Natl. Acad Sci. U.S.A. 83*, 342-346.
Rill, R. L., Hilliard, P. R., & Levy, G. C. (1983) *J. Biol. Chem. 258*, 250-256.
Robinson, C. (1961) *Tetrahedron 13*, 219-234.
Roy, S., Hiyama, Y., Torchia, D. A., & Cohen, J. S. (1986) *J. Am. Chem. Soc. 108*, 1675-1678.
Saenger, W. (1984) in *Principles of Nucleic Acid Structure*, Springer-Verlag, New York.
Santos, R. A., Tang, P., & Harbison, G. S. (1989) *Biochemistry 28*, 9372-9378.
Shindo, H., Fujiwara, T., Akustu, H., Matsumoto, U., & Kyogoku, Y. (1985) *Biochemistry 24*, 887-895.
Shindo, H., Hiyama, Y., Roy, S., Cohen, J. S., & Torchia, D. A. (1987) *Bull. Chem. Soc. Jpn. 60*, 1631-1640.
Stewart, P. L., Valentine, K. G., & Opella, S. J. (1987) *J. Magn. Reson. 71*, 45-61.
Tsang, P., Vold, R. R., & Vold, R. L. (1987) *J. Magn. Reson. 71*, 276-282.
Vold, R. R., Brandes, R., Tsang, P., Kearns, D. R., & Vold, R. L. (1986) *J. Am Chem. Soc. 108*, 302-303.
Wing, R., Drew, H., Takano, T., Broka, C., Tanaka, S., Itakura, K., & Dickerson, R. E. (1980) *Nature 287*, 755-758.

Resonance Raman Spectroscopic Characterization of Compound III of Lignin Peroxidase†

Muthusamy Mylrajan,‡ Khadar Valli, Hiroyuki Wariishi, Michael H. Gold,* and Thomas M. Loehr*
Department of Chemical and Biological Sciences, Oregon Graduate Institute of Science and Technology, 19600 N.W. von Neumann Drive, Beaverton, Oregon 97006-1999
Received May 4, 1990; Revised Manuscript Received July 9, 1990

ABSTRACT: Resonance Raman (RR) spectra of several compounds III of lignin peroxidase (LiP) have been measured at 90 K with Soret and visible excitation wavelengths. The samples include LiPIIIa (or oxyLiP) prepared by oxygenation of the ferrous enzyme, LiPIIIb generated by reaction of the native ferric enzyme with superoxide, LiPIIIc prepared from native LiP plus H_2O_2 followed by removal of excess peroxide with catalase, and LiPIII* made by addition of excess H_2O_2 to the native enzyme. The RR spectra of these four products appear to be similar and, thus, indicate that the environments of these hexacoordinate, low-spin ferriheme species must also be very similar. Nonetheless, the Soret absorption band of LiPIII* is red-shifted by 5 nm from the 414-nm maximum common to LiPIIIa, -b, and -c [Wariishi, H., & Gold, M. H. (1990) *J. Biol. Chem. 265*, 2070-2077]. Analysis of the iron-porphyrin vibrational frequencies indicates that the electronic structures for the various compounds III are consistent with an $Fe^{III}O_2^{\bullet -}$ formulation. The spectral changes observed between the oxygenated complex and the ferrous heme of lignin peroxidase are similar to those between oxymyoglobin and deoxymyoglobin. The contraction in the core sizes in compound III relative to the native peroxidase is analyzed and compared with that of other heme systems. EPR spectra confirm that the high-spin ferric form of the native enzyme, with an apparent $g = 5.83$, is converted into the EPR-silent LiPIII* upon addition of excess H_2O_2. Its magnetic behavior may be explained by antiferromagnetic coupling between the low-spin Fe^{III} and the superoxide ligand. The Fe–O_2 stretching vibration of the oxygenated peroxidase is observed at 563 cm^{-1} and shifts to 538 cm^{-1} with ^{18}O isotope. The Fe–histidine stretching vibration is observed at 245 cm^{-1} in ferrous peroxidase and appears to shift to 276 cm^{-1} in the oxygenated complex.

Phanerochaete chrysosporium, a white rot basidiomycete, is capable of degrading lignin, a heterogeneous phenylpropanoid polymer comprising 15-25% of woody plant cell walls (Gold et al., 1989; Kirk & Farrell, 1987; Buswell & Odier, 1987). Under secondary metabolic growth conditions, this fungus secretes two extracellular, H_2O_2-dependent heme enzymes, lignin peroxidase (LiP)[1] and manganese peroxidase (MnP), that are involved in lignin degradation (Gold et al., 1989; Kirk & Farrell, 1987; Buswell & Odier, 1987). LiP has

† This research was supported by grants from the National Institutes of Health (GM 18865 and GM 34468 to T.M.L.), the National Science Foundation (DMB 8904358 to M.H.G.), and the U.S. Department of Energy (DE-FG-06-87ER13715 to M.H.G.). The support of the NIH is further acknowledged for awards through its Biomedical Research Support Grant (S07 RR 07184) and Shared Instrumentation Grant (S10 RR 01482 and S10 RR 02676) programs used toward the purchase of research instrumentation used in this work.
* To whom correspondence should be addressed.
‡ Visiting Postdoctoral Research Associate from the Indian Institute of Technology, Madras 600036, India.

[1] Abbreviations: LiP, lignin peroxidase; LiPIII, lignin peroxidase compound III; CCP, cytochrome *c* peroxidase; DHF, dihydroxyfumarate; EPR, electron paramagnetic resonance; HRP, horseradish peroxidase; Im, imidazole; LPO, lactoperoxidase; MnP, manganese peroxidase; oxyHb, oxyhemoglobin; oxyLiP, same as LiPIIIa; oxyMb, oxymyoglobin; PP, protoporphyrin; RR, resonance Raman; RZ, Reinheitszahl = A_{407}/A_{280}.

0006-2960/90/0429-9617$02.50/0

been purified to homogeneity and characterized spectroscopically (Gold et al., 1989, 1984; Tien, 1987; Andersson et al., 1985, 1987; Kuila et al., 1985; Renganathan & Gold, 1986; Marquez et al., 1988). LiP is a glycoprotein of M_r = 41 000 with one iron protoporphyrin IX prosthetic group. Native LiP exists predominately as a high-spin, pentacoordinate Fe^{III} heme with a histidine coordinated as fifth ligand as evidenced by electronic absorption, resonance Raman (RR), and electron paramagnetic resonance (EPR) spectroscopy (Gold et al., 1984; Andersson et al., 1985, 1987; Kuila et al., 1985). LiP has a pH optimum at ~3.0 (Gold et al., 1989; Kirk & Ferrell, 1987; Buswell & Odier, 1987; Tien, 1987) and catalyzes the H_2O_2-dependent oxidation of lignin model compounds (Gold et al., 1989; Kirk & Farrell, 1987; Buswell & Odier, 1987) via the initial formation of a substrate aryl cation radical with subsequent nonenzymatic reactions to yield a variety of degradation products. Electronic absorption spectra of the oxidized forms of LiP compounds I–III have been reported (Gold et al., 1989; Renganathan & Gold, 1986; Marquez et al., 1988; Wariishi & Gold, 1989, 1990; Harvey et al., 1989). Compound I has an Fe^{IV}=O, porphyrin π-cation radical structure, whereas compound II resides as an Fe^{IV}=O, porphyrin structure (Renganathan & Gold, 1986; Marquez et al., 1988; Dunford & Stillman, 1976). Compound III can be formed by three different methods (Wariishi & Gold, 1990; Dunford & Stillman, 1976): LiPIIIa is made by oxygenation of Fe^{II}LiP to form the ferrous oxy species; this species is also referred to as oxyLiP in parallel with the oxygenated forms of other heme proteins. LiPIIIb is produced by the addition of $O_2^{\bullet -}$ to native LiP, whereas LiPIIIc is prepared by the addition of ~40 equiv of H_2O_2 to native LiP followed by the removal of excess H_2O_2 with catalase. Although compound III of LiP is not involved in the normal peroxidase catalytic cycle (Wariishi & Gold, 1990; Dunford & Stillman, 1976; Yamazaki, 1974), it can lead to the inactivation of the enzyme (Wariishi & Gold, 1989, 1990). In the presence of excess H_2O_2, LiPIII* is formed, a species that reacts with H_2O_2 to be inactivated with concomitant bleaching of the heme spectrum (Wariishi & Gold, 1989, 1990). The ready conversion of LiPIII* to the native form of the enzyme upon the addition of veratryl alcohol, a *P. chrysosporium* secondary metabolite, explains this alcohol's role in stabilizing the enzyme in the presence of excess H_2O_2 (Wariishi & Gold, 1990). In the present paper, RR and EPR studies of various compounds III are reported whose formation is summarized by the reactions:

$$\text{ferrous LiP} + O_2 \rightarrow \text{LiPIIIa}$$

$$\text{native LiP} + O_2^{\bullet -} \rightarrow \text{LiIIIb}$$

$$\text{native LiP} + \text{xs } H_2O_2 \rightarrow \text{LiPIII*}$$

$$\text{LiPIII*} + \text{catalase} \rightarrow \text{LiPIIIc}$$

Materials and Methods

Enzyme Preparations. The major isozyme of lignin peroxidase (LiP-2) was purified from the extracellular medium of acetate-buffered, agitated cultures of *P. chrysosporium* as previously described (Gold et al., 1984; Wariishi & Gold, 1990). The purified protein was electrophoretically homogeneous and had an RZ $\simeq$ 5.0. Enzyme concentrations were determined at 407.6 nm by using a molar absorptivity of 133 mM^{-1} cm^{-1} (Gold et al., 1984). The enzyme was dialyzed exhaustively against buffer before use.

Chemicals. H_2O_2 (30% solution) was purchased from Aldrich. The concentration of H_2O_2 was determined as previously reported (Cotton & Dunford, 1973). Dihydroxyfumaric acid (DHF) and catalase were obtained from Sigma. All other chemicals were of reagent grade. Solutions were prepared with deionized water obtained from a Milli Q (Millipore) system.

Preparation of Samples for Raman Spectroscopy. (*A*) *LiPIIIa (Ferrous–Oxy Complex).* Ferrous LiP was prepared by addition of ~30 equiv of sodium dithionite to ~250 μM native LiP in 50 mM sodium succinate, pH 4.5, under anaerobic conditions (Gold et al., 1984). Deuterium-exchanged Fe^{II}LiP was prepared by three dilution/concentration cycles of native LiP in a 2-fold volume excess of D_2O (Sigma, 99.8 atom %) over 72 h before reduction. LiPIIIa was generated by purging the ferrous enzyme with oxygen as previously reported (Renganathan & Gold, 1986; Wariishi & Gold, 1990).

(*B*) *LiPIIIb (Ferric–Superoxide Complex).* LiPIIIb was prepared by successive addition of 20 equiv of DHF and 1 equiv of H_2O_2 to ~250 μM native enzyme in 50 mM sodium succinate, pH 4.5 (Wariishi et al., 1990). During the aerobic oxidation of DHF to diketosuccinate by HRP, the generation of superoxide ion has been reported; the $O_2^{\bullet -}$ in turn reacts with native HRP to form compound III (Yamazaki & Piette, 1963; Halliwell, 1978). The addition of only 1 equiv of H_2O_2 stimulates the peroxidase oxidation of DHF to its radical form (Yamazaki & Piette, 1963; Wariishi et al., 1990). After the formation of LiPIIIb was confirmed spectrophotometrically, a catalytic amount of catalase (0.01 equiv) was immediately added to decompose H_2O_2 generated through the disproportionation of $O_2^{\bullet -}$.

(*C*) *LiPIII* and LiPIIIc.* LiPIII* was prepared by addition of ~40 equiv H_2O_2 to ~250 μM native LiP in 50 mM sodium succinate, pH 4.5 (Renganathan & Gold, 1986; Marquez et al., 1988; Wariishi & Gold, 1989, 1990). Addition of 0.01 equiv of catalase to LiPIII* to remove excess H_2O_2 resulted in its conversion to LiPIIIc as previously reported (Wariishi & Gold, 1990). Absorption spectra showed that the Soret maxima of LiPIIIa, -b, and -c were all at 414 nm, whereas that of LiPIII* was at 419 nm.

Electronic absorption spectra were recorded at room temperature on a Shimadzu UV-260 spectrophotometer operated with a spectral bandwidth of 1.0 nm and 1.0-cm cells. Resonance Raman spectra were obtained with computer-controlled Dilor Z24 and Jarrell-Ash 25-300 Raman spectrophotometers. Spectra-Physics 2025-11 Kr and Coherent Innova 90-6 Ar lasers were used to generate 413.1- and 514.5-nm excitation wavelengths. Since LiP compound III species held close to ambient temperatures (~275–295 K) showed evidence of degradation during data collection, we resorted to cryogenic methods where the sample is maintained at ~90 K in a cold-finger Dewar and probed in a backscattering geometry as previously reported (Andersson et al., 1985, 1987). Unless otherwise indicated, all RR spectra were obtained from samples at 90 K. Absorption spectra were recorded after the RR measurements to ensure the integrity of compound III species, whose stabilities at 90 K are considerably higher than at ~280 K. For example, LiPIII* is converted to the native form upon laser illumination at 280 K, although even after 3 h in the laser beam at 90 K, this sample was found to be largely intact. Raman spectrometers were calibrated with standard indene frequencies (Hendra & Loader, 1968). X-band EPR spectra were obtained as described previously on a Varian E-109 spectrometer equipped with an Air Products liquid helium cryostat (Andersson et al., 1985). The magnetic field was calibrated with strong pitch.

Results and Discussion

High-Frequency (1300–1700-cm^{-1}) Region. Resonance

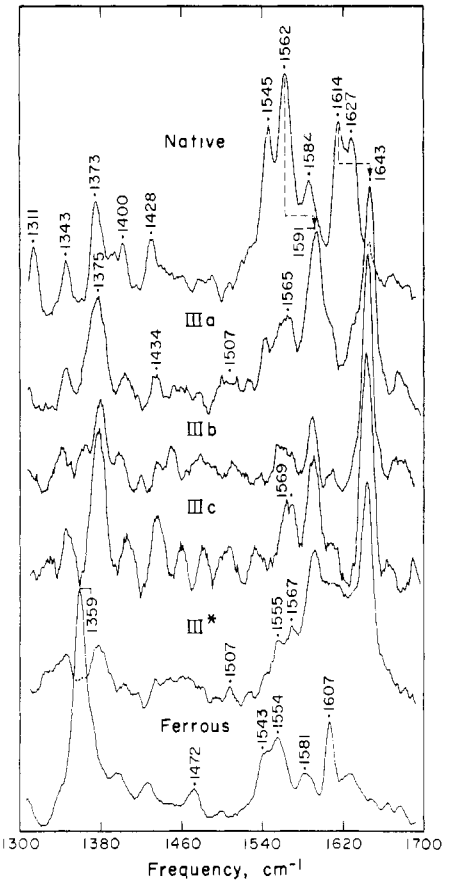

FIGURE 1: Resonance Raman spectra (1300–1700 cm^{-1}) of native LiP, LiPIII (a–c), LiPIII*, and ferrous LiP. LiP (~250 μM) in 50 mM sodium succinate buffer pH 4.5. Conditions: 514.5-nm excitation; laser power at the sample 20 mW; slit width 5 cm^{-1}; scan speed 1 cm^{-1}/s with repetitive scanning. Sample temperature is ~90 K for all samples except ferrous LiP (273 K).

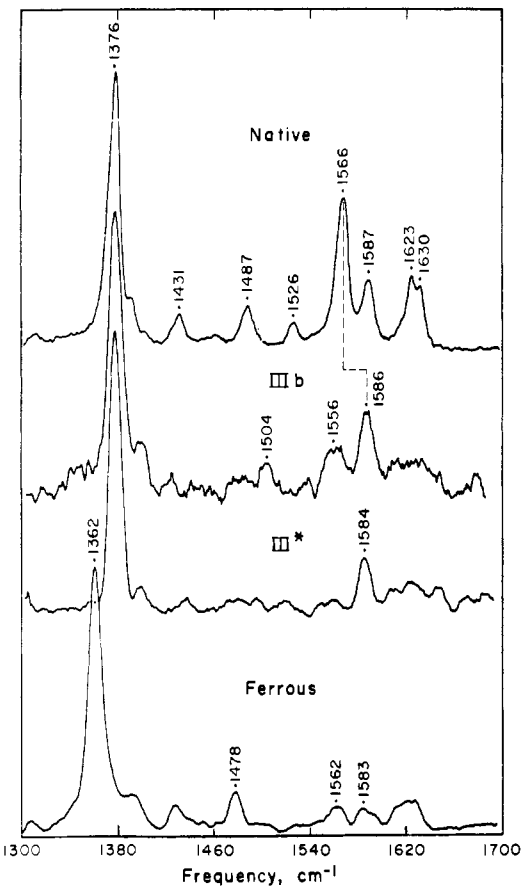

FIGURE 2: Resonance Raman spectra (1300–1700 cm^{-1}) of native LiP, LiPIIIb, LiPIII*, and ferrous LiP. Conditions: 413.1-nm excitation; laser power 10 mW; sample temperature 90 K; other conditions as in Figure 1.

Table I: Resonance Raman Frequencies and Assignments for Various Preparations of LiP Compound III Compared with Oxyhemoglobin and Oxyhorseradish Peroxidase

	compound III–LiP[a]					
mode (ρ)[b]	IIIa	IIIb	IIIc	III*	oxyHb[c]	oxyHRP[d]
ν_{10} (dp)	1643	1643	1643	1642	1640	1640
ν(C=C) (2) (p)			*e*			1637
ν(C=C) (1) (p)			*e*		1620	
ν_{37} (p)	1605	1606	1604	1607	1606	1601
ν_{19} (ap)	1591	1589	1591	1593	1586	1585
ν_2 (p)	1586	1586	1584	1586	1583	1582
ν_{11} (dp)	1565	1567	1569	1569	1564	1564
ν_{38} (dp)	1556	1556	1555	1557	1552	1543
ν_3 (p)	1507	1504	1507	1509	1506	1506
ν(=CH_2) (dp)	1434	1436	1434	1436	1431	1430
ν_{29} (dp)	1404	1399	1403	1408	1400	1399
ν_4 (p)	1378	1379	1378	1378	1377	1378

[a] This work; data from Soret and visible excitation spectra. [b] Mode identifications from Abe et al. (1978); for vinyl mode assignments, see text. Expected depolarization (ρ): p = polarized, dp = depolarized, ap = anomalously polarized. [c] Spiro and Strekas (1974). [d] Van Wart and Zimmer (1985). [e] Native LiP shows two strong bands at 1623 and 1630 cm^{-1} (see Figure 2); LiPIII species appear to have two weak vinyl bands at similar frequencies.

Raman spectra of lignin peroxidase compounds III (forms IIIa, IIIb, and IIIc) and compound III*, as well as those of native and ferrous LiP obtained with Q-band excitation at 514.5 nm, are shown in Figure 1. Selected spectra obtained with Soret excitation at 413.1 nm are given in Figure 2. Frequencies and assignments of the prominent bands are given in Table I. The high degree of similarity of the four compound III RR spectra, within the signal-to-noise limits of the present data, argues that the heme prosthetic groups of the LiPIII species formed under different reaction conditions are effectively indistinguishable and that their heme environments possess identical spin and oxidation states.[2] In particular, these data are consistent with an earlier suggestion that LiPIII* is a simple association complex between the LiPIII form of the enzyme and H_2O_2 (Wariishi & Gold, 1990). These data, as well as earlier spectral data (Wariishi & Gold, 1990), contrast with the assertion that the addition of H_2O_2 to LiPIII results in the formation of LiP compound II (Cai & Tien, 1989).[3] Spectra obtained with Soret excitation predominately show enhancement of the totally symmetric (polarized) modes of vibrations of the heme group (Figure 2), whereas excitation within the "visible" range enhances depolarized and anomalously polarized bands (Figure 1; Spiro, 1983, 1985).

Spin-State Bands. Resonance Raman bands that reflect the spin state of the heme are ν_3, ν_{10}, and ν_{19} (Spiro, 1983; Felton & Yu, 1978); the latter two are generally more prom-

[2] The RR spectrum of III* differs most among the set of spectra of various compound III preparations shown in Figure 1. This species has a known propensity for decomposition in the presence of excess H_2O_2. Additionally, III* also reverts to native LiP that has prominent RR bands in the 1540–1630-cm^{-1} range and could account for the spectral intensity of III* in that region as observed with visible excitation.

[3] Compound II species of peroxidases have an intense band at ~790 cm^{-1} assigned to their Fe^{IV}=O stretching modes (Sitter et al., 1986). In none of our RR spectra of the various LiP compound III species could we detect a peak at this frequency, and we concluded that our preparations of III contained no compound II. Moreover, the optical spectra of samples of III obtained *after* recording their RR spectra also indicated the absence of LiP compound II.

inent with Q-band excitation, of which ν_{10} is most easily distinguished because it is the most prominent high-frequency band. For example, the six-coordinate, low-spin ferric hemes in CN^-–metMb, CN^-–LiP, and Im_2FePP have their ν_{10} bands at 1642, 1639, and 1640 cm^{-1}, respectively (Andersson et al., 1985; Rakshit & Spiro, 1974). As seen in Figure 1, the spectra of LiPIII and LiPIII* have a very prominent new band at $\sim$1643 cm^{-1} that we assign to ν_{10}. The $\sim$30-cm^{-1} shift in ν_{10} from 1614 cm^{-1} in the native high-spin ferric form to 1643 cm^{-1} clearly indicates that LiPIII and LiPIII* are six-coordinate, low-spin species. Similarly, ν_{10} of compound III of HRP is also observed at $\sim$1640 cm^{-1} (Van Wart & Zimmer, 1985; Palaniappan & Terner, 1989).

The polarized spin-state marker band ν_3 appears in the region 1497-1508 cm^{-1} in authentic hexacoordinate, low-spin ferric heme systems such as CN^- and N_3^- complexes of LiP and metHb (Andersson et al., 1985), MnP (Mino et al., 1988), HRP (Rakshit & Spiro, 1974), and CCP (Sievers et al., 1979). In native LiP (hs, 5-coord), this frequency is at 1487 cm^{-1} and shifts to $\sim$1505 cm^{-1} on formation of compound III (Table I), clearly indicating conversion to a low-spin species. The prominent ν_{19} (ap) mode appearing at 1562 cm^{-1} in the native form with 514.5-nm excitation shifts to 1591 cm^{-1} in compound III species (Figure 1). The $\sim$30-cm^{-1} upshift of the ν_{19} mode upon formation of compound III species is similarly consistent with the behavior of other ferrihemes experiencing this change in spin state (Spiro, 1983; Felton & Yu, 1978; Mino et al., 1988).

Oxidation-State Marker. The C_a–N mode ν_4 has long been known to be sensitive to the oxidation state of the heme moiety (Spiro & Strekas, 1974; Spiro, 1983). More recently, this characteristic band has been termed an electron density indicator (Spiro & Li, 1988), because it reflects the electron population in the porphyrin π^* orbitals. When the electron population in the π^* orbitals is increased by back-donation from the iron $d\pi$ orbitals, as in the case of ferrous hemes, the porphyrin bonds weaken and thereby the vibrational frequency decreases. Band ν_4 is observed at 1373 cm^{-1} in native LiP and makes only a slight upshift to $\sim$1375 cm^{-1} in compound III with 514.5-nm excitation (Figure 1); with 413.1-nm excitation (Figure 2), ν_4 appears at 1376 cm^{-1} in the native form and also shows a shift up to $\sim$1378 cm^{-1} in compound III species. The frequency positions of this heme system are indicative of the Fe^{III} oxidation state. In contrast, ν_4 for ferrous LiP is at $\sim$1360 cm^{-1} (Figures 1 and 2). The electronic structures of compound III and compound III* are thus formally consistent with a ferric–superoxide, $Fe^{III}O_2^{\bullet -}$, formulation.

Vinyl Modes. In native LiP, two overlapped bands are seen at $\sim$1622 and 1629 cm^{-1} (280 K, data not shown), but at 90 K, these bands become distinct at 1623 and 1630 cm^{-1} (Figure 2). These two bands may be assigned to C=C stretching modes of the two vinyl substituents. Comparable bands have been observed at $\sim$1620 and 1630 cm^{-1} in several HRP derivatives using near-UV excitation (Palaniappan & Terner, 1989) and in CCP using 413-nm excitation (Dasgupta et al., 1989). According to the normal coordinate analysis of Lee et al. (1986), an $\sim$10-cm^{-1} splitting between the vinyl stretching modes has been predicted. Since the intensity contribution by ν_{10} is expected to be very weak with Soret excitation wavelengths, we favor assignment of the observed $\sim$1620/1630 cm^{-1} pair to these vinyl modes.

In LiPIII and LiPIII* (Figure 2) these vinyl bands are unexpectedly weak with Soret excitation but appear to be present at approximately identical frequencies to those of native LiP. Polarized RR bands have been reported at 1620 cm^{-1} in oxyMb (Spiro & Strekas, 1974) and at 1637 cm^{-1} in oxyHRP (Van Wart & Zimmer, 1985) that are presumably due to vinyl modes (Table I).

Core Size Correlations. The high-frequency porphyrin skeletal modes are sensitive to the degree of core expansion in the porphyrin macrocycle. Spaulding et al. (1975) first noted a linear dependence of one of the high-frequency RR bands on the core size in a series of metallooctaethyl porphyrins. Later, Huong and Pommier (1977) found a core size dependence for two other bands. Spiro and co-workers subsequently analyzed relative effects of core size and doming on RR frequencies and extended the analysis of the core size to all the skeletal modes (Spiro et al., 1979; Choi et al., 1982; Parthasarathi et al., 1987). All skeletal modes above 1350 cm^{-1} show negative linear dependence on center-to-nitrogen (C_t–N) distance. In protoporphyrins, the C_a–C_m modes show large slopes compared to C_b–C_b modes, reflecting the greater sensitivity of the former to core size. On the basis of the empirical relation $\nu = k(A - d)$, where d = core size (in Å), k = reciprocal slope, and A = intercept, the core size expansion and contraction can be calculated.

In deoxyMb, the Fe^{II} is out of plane by 0.55 Å from the mean tetrapyrrole plane; the heme group is domed, and the proximal histidine is tilted away from the normal (Takano, 1977). In oxyMb, the Fe lies much closer to the heme plane (0.19 Å), the heme group is nearly planar, and the proximal histidine is nearly normal to the heme plane (Norvell et al., 1975; Phillips, 1980). Similar movement of the Fe atom is expected between the ferrous and compound III forms of LiP. The contraction of the core gives increases in the core size marker bands whereas the opposite is true for an expanded core. A value for the C_t–N distance in native Fe^{III}LiP of 2.034 Å may be calculated from the average of the values determined from selected frequencies: ν_3 (2.023 Å), ν_{19} (2.033 Å), and ν_{10} (2.046 Å). For the ferrous form, C_t–N is calculated to be 2.053 Å (average of 2.061, 2.053, and 2.045 Å from ν_3, ν_{19}, and ν_{10}, respectively). The larger value in the Fe^{II} enzyme is consistent with the larger ionic radius of the reduced metal.

Upon formation of LiP compound III, the out-of-plane Fe moves into the plane, and the core size is reduced to 1.978 Å as determined from the new core size frequencies. This number is close to the C_t–N values of 1.980 and 1.985 Å calculated from the frequencies given for oxyMb (Spiro & Strekas, 1974) and oxyHb (Van Wart & Zimmer, 1985), respectively. The data in Table I permit a core size calculation for oxyHRP of 1.985 Å. In the case of oxyLiP, the core size is contracted by 0.056 Å from that of ferric LiP and 0.075 Å from that of ferrous LiP.

Low-Frequency RR Data. The RR spectra of the low-frequency region provide additional information on the heme environment where the Fe–axial ligand stretching modes are expected to appear. Figure 3 compares native and ferrous LiP spectra with those from LiPIIIa. The major differences appear to be in intensities rather than frequencies. Figure 4 shows spectra of LiPIIIb in the region of the Fe–O_2 stretching region identified here by oxygen isotope substitution.

Fe–N(Histidine) Stretching Modes. In deoxyMb and deoxyHb, the Fe–N(His) axial ligand vibration has been identified at $\sim$220 cm^{-1} (Kitagawa et al., 1979; Kincaid et al., 1979; Nagai et al., 1980), and at 245 cm^{-1} for HRP (Teraoka & Kitagawa, 1981; Teraoka et al., 1983; Kitagawa et al., 1983) with isotopic substitution of iron. Ferrous LiP has a prominent band at $\sim$245 cm^{-1} (Kuila et al., 1985; Figure 3) which is assigned to the Fe–N(His) mode; however, we failed to detect any shift of this band following D_2O exchange. A

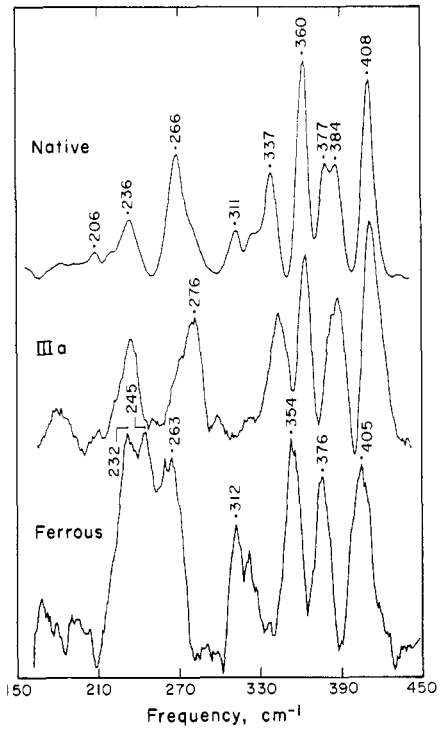

FIGURE 3: Resonance Raman spectra (150–450 cm^{-1}) of native LiP, LiPIIIa, and ferrous LiP. Conditions: 413.1-nm excitation; laser power 10 mW; other conditions as in Figure 1. Sample temperature is ~90 K for all samples except ferrous LiP (273 K).

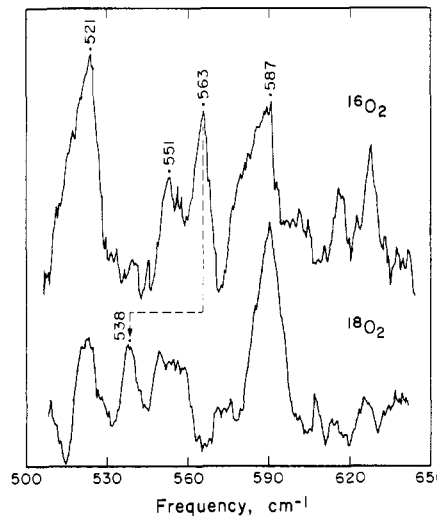

FIGURE 4: Resonance Raman spectra (500–650 cm^{-1}) of LiPIIIb (native + $O_2^{\bullet -}$ form) prepared via the DHF + O_2 reaction. (Top) With $^{16}O_2$; (bottom) with $^{18}O_2$. Conditions: 413.1-nm excitation; laser power at the sample 4 mW; slit width 8 cm^{-1}; other conditions as in Figure 1.

proximal histidine ligand in both LiP and MnP has been confirmed by comparing the sequence of their cDNAs with the sequence of other plant and fungal peroxidases (Tien & Tu, 1987; Pribnow et al., 1989). For myoglobin, an ~2-cm^{-1} downward shift upon D_2O substitution has been reported (Kincaid et al., 1979). The Fe–N(His) stretch also has been identified at 248 cm^{-1} in reduced manganese peroxidase (Mino et al., 1988). The high Fe–N(His) stretching frequency in ferrous HRP has been attributed to its strongly hydrogen-bonded histidine (Teraoka & Kitagawa, 1981). The crystal structure of CCP reveals that its proximal His-175 is hydrogen bonded to a buried Asp-235 with a bond length of 2.9 Å (Finzel et al., 1984). In globins, the proximal histidine is

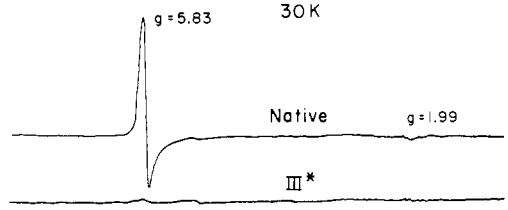

FIGURE 5: Electron paramagnetic resonance spectra of native LiP and LiPIII*. Spectra obtained at 30 K from a single sample of 200 μL of 50 μM native LiP (upper) to which 20 μL of 20 mM H_2O_2 was added to obtain III* (lower curve).

hydrogen bonded to a peptide backbone C=O with a typical bond length of ~2.7 Å (Valentine et al., 1979). The higher Fe–N(His) stretching frequencies in HRP, MnP, and LiP indicate their greater Fe–N bond strengths that are due, in part, to stronger hydrogen bonding of the proximal histidines. A similarly high Fe–N(histidine) stretching vibration has been reported at ~255 cm^{-1} for the mammalian lactoperoxidase (Manthey et al., 1986).

Typically, Fe–N(His) stretching bands are detected on the reduced ferrous hemes; intensities in ferrihemes and oxygenated species are very low and, consequently, hard to detect. Walters and Spiro (1982) have assigned a shoulder at 271 cm^{-1} in RR spectra of oxyMb to this mode. The feature at ~275 cm^{-1} that appears as a shoulder on the 266-cm^{-1} band may be the Fe–N(His) stretching mode in native LiP. LiPIIIa also has a band at 276 cm^{-1} (Figure 3), as well as LiPIIIc and LiPIII*; these bands at ~276 cm^{-1} may have a contribution from the Fe–N(His) stretching modes. These bands appear with equal intensity to that of the 266-cm^{-1} band of native LiP.

Fe–O_2 Stretching Vibration. Figure 4 shows RR data obtained from LiP compound IIIb prepared via the DHF/O_2 reaction using normal O_2 and isotopically enriched $^{18}O_2$. These experiments were extremely difficult to perform because of the photolability of the product, even at 90 K. Only with very low laser power could data be obtained that show the Fe–O_2 stretching modes. The band observed at 563 cm^{-1} in the ^{16}O species of LiPIIIb shifts to 538 cm^{-1} in the ^{18}O-substituted enzyme. These band positions agree very well with those observed at 570 cm^{-1} for oxyMb (Van Wart & Zimmer, 1985; Tsubaki et al., 1980) and at 562 cm^{-1} for oxyHRP (Van Wart & Zimmer, 1985).

The Fe–O_2 stretching mode was first reported by Brunner (1974) at 567 cm^{-1} for oxyHb; it shifts to 540 cm^{-1} with the ^{18}O adduct. The Fe–O_2 stretching frequencies of the oxygen complex of "picket fence" synthetic porphyrins (Burke et al., 1978) also show bands at 568 cm^{-1} with $^{16}O_2$ and at 545 cm^{-1} with $^{18}O_2$. All observed isotope shifts are similar in magnitude and agree well with the values that can be calculated from mass considerations for simple oscillators.

EPR Spectra. The EPR spectrum of native LiP is consistent with a high-spin system (Andersson et al., 1985), but the EPR spectrum of LiPIII* is silent (Figure 5). The spin-coupled nature can be explained by an antiferromagnetic interaction between the unpaired electron of the low-spin Fe^{III} ion and that of the coordinated superoxide ion. Mössbauer spectra (Schulz et al., 1984) of compound III of HRP show a quadrupole doublet with a splitting of $\Delta E_Q = -2.3$ mm/s and an isomer shift $\delta = 0.23$ mm/s at 4.2 K which are similar to other oxyheme complexes. The Mössbauer spectra of HRP compound III in high field have been interpreted as arising from an $S = 0$ ground state. In small applied fields, no magnetic interaction is evident as expected for an integer spin system. The EPR data for LiPIII* are also consistent with a diamagnetic ground state.

Conclusions

Detailed RR spectral studies of compound III of LiP reveal that it is a low-spin hexacoordinate system with iron formally in the Fe^{III} state. The spectral data are very similar to those of oxyHRP and oxyMb. Preparations of LiPIII and LiPIII* formed via a variety of reactions give essentially identical RR spectra and are judged to be similar in their heme electronic structures. These data are consistent with an earlier suggestion (Wariishi & Gold, 1990; Wariishi et al., 1990) that LiPIII* is a simple association complex between the LiPIII form of the enzyme and H_2O_2. The core size of LiPIII is contracted when compared to ferrous LiP and native LiP and is consistent with an in-plane, diamagnetic metalloporphyrin structure that is EPR silent. The Fe–O_2 stretching band at 563 cm^{-1} shifts to 538 cm^{-1} on ^{18}O isotope substitution.

References

Abe, M., Kitagawa, T., & Kyogoku, Y. (1978) *J. Chem. Phys. 69*, 4526–4534.

Andersson, L. A., Renganathan, V., Chiu, A. A., Loehr, T. M., & Gold, M. H. (1985) *J. Biol. Chem. 260*, 6080–6087.

Andersson, L. A., Renganathan, V., Loehr, T. M., & Gold, M. H. (1987) *Biochemistry 26*, 2258–2263.

Brunner, H. (1974) *Naturwissenschaften 61*, 129.

Burke, J. M., Kincaid, J. R., Peters, S., Gagne, R. R., Collman, J. P., & Spiro, T. G. (1978) *J. Am. Chem. Soc. 100*, 6083–6088.

Buswell, J. A., & Odier, E. (1987) *CRC Crit. Rev. Biotechnol. 6*, 1–60.

Cai, D., & Tien, M. (1989) *Biochem. Biophys. Res. Commun. 162*, 464–469.

Choi, S., Spiro, T. G., Langry, K. C., & Smith, K. M. (1982) *J. Am. Chem. Soc. 104*, 4337–4344.

Cotton, H. L., & Dunford, H. B. (1973) *Can. J. Chem. 51*, 582–587.

Dasgupta, S., Rousseau, D. L., Anni, H., & Yonetani, T. (1989) *J. Biol. Chem. 264*, 654–662.

Dunford, H. B., & Stillman, J. S. (1976) *Coord. Chem. Rev. 19*, 187–251.

Felton, R. H., & Yu, N.-T. (1978) in *The Porphyrins* (Dolphin, D., Ed.) Vol. 3, pp 347–393, Academic Press, New York.

Finzel, B. C., Poulos, T. L., & Kraut, J. (1984) *J. Biol. Chem. 259*, 13027–13036.

Gold, M. H., Kuwahara, M., Chiu, A. A., & Glenn, J. K. (1984) *Arch. Biochem. Biophys. 234*, 353–362.

Gold, M. H., Wariishi, H., & Valli, K. (1989) in *ACS Symposium on Biocatalysis in Agricultural Biotechnology* (Whitaker, J. R., & Sonnet, P., Eds.) Ser. No. 389, pp 127–140, American Chemical Society, Washington, DC.

Halliwell, B. (1978) *Planta 140*, 81–88.

Harvey, P. J., Palmer, J. M., Shoemaker, H. E., Dekker, H. L., & Wever, R. (1989) *Biochim. Biophys. Acta 994*, 59–63.

Hendra, P. J., & Loader, E. (1968) *Chem. Ind. (London)* 718–719.

Huong, P. V., & Pommier, J.-C. (1977) *C. R. Acad. Sci. Ser. C 285*, 519–522.

Kincaid, J., Stein, P., & Spiro, T. G. (1979) *Proc. Natl. Acad. Sci. U.S.A. 76*, 549–552, 4156 (errata).

Kirk, T. K., & Farrell, R. L. (1987) *Annu. Rev. Microbiol. 41*, 465–505.

Kitagawa, T., Nagai, K., & Tsubaki, M. (1979) *FEBS Lett. 104*, 376–378.

Kitagawa, T., Hashimoto, S., Teraoka, J., Nakamura, S., Yajima, H., & Hosoya, T. (1983) *Biochemistry 22*, 2788–2792.

Kuila, D., Tien, M., Fee, J. A., & Ondrias, M. R. (1985) *Biochemistry 24*, 3394–3397.

Lee, H., Kitagawa, T., Abe, M., Pandey, R. K., Leung, H.-K., & Smith, K. M. (1986) *J. Mol. Struct. 146*, 329–347.

Manthey, J. A., Boldt, N. J., Bocian, D. F., & Chan, S. I. (1986) *J. Biol. Chem. 261*, 6734–6741.

Marquez, L., Wariishi, H., Dunford, H. B., & Gold, M. H. (1988) *J. Biol. Chem. 263*, 10549–10552.

Mino, Y., Wariishi, H., Blackburn, N. J., Loehr, T. M., & Gold, M. H. (1988) *J. Biol. Chem 263*, 7029–7036.

Nagai, K., Kitagawa, T., & Morimoto, H. (1980) *J. Mol. Biol. 136*, 271–289.

Norvell, J. C., Nunes, A. C., & Schoenborn, B. P. (1975) *Science 190*, 568–570.

Palaniappan, V., & Terner, J. (1989) *J. Biol. Chem. 264*, 16046–16051.

Parthasarathi, N., Hansen, C., Yamaguchi, S., & Spiro, T. G. (1987) *J. Am. Chem. Soc. 109*, 3865–3871.

Phillips, S. E. V. (1980) *J. Mol. Biol. 142*, 531–554.

Pribnow, D., Mayfield, M. B., Nipper, V. J., Brown, J. A., & Gold, M. H. (1989) *J. Biol. Chem. 264*, 5036–5040.

Rakshit, G., & Spiro, T. G. (1974) *Biochemistry 13*, 5317–5323.

Renganathan, V., & Gold, M. H. (1986) *Biochemistry 25*, 1626–1631.

Schulz, C. E., Rutter, R., Sage, J. T., Debrunner, P. G., & Hager, L. P. (1984) *Biochemistry 23*, 4743–4754.

Sievers, G., Osterlund, K., & Ellfolk, N. (1979) *Biochim. Biophys. Acta 581*, 1–14.

Sitter, A. J., Reczek, C. M., & Terner, J. (1986) *J. Biol. Chem. 261*, 8638–8642.

Spaulding, L. D., Chang, C. C., Yu, N.-T., & Felton, R. H. (1975) *J. Am. Chem. Soc. 97*, 2517–2525.

Spiro, T. G. (1983) in *Iron Porphyrins* (Lever, A. B. P., & Gray, H. B., Eds.) Part II, pp 91–159, Addison-Wesley, Reading, MA.

Spiro, T. G. (1985) *Adv. Protein Chem. 37*, 111–159.

Spiro, T. G., & Strekas, T. C. (1974) *J. Am. Chem. Soc. 96*, 338–345.

Spiro, T. G., & Li, X.-Y. (1988) in *Biological Applications of Raman Spectroscopy* (Spiro, T. G., Ed.) Vol. 3, pp 1–37, John Wiley & Sons, New York.

Spiro, T. G., Stong, J. D., & Stein, P. (1979) *J. Am. Chem. Soc. 101*, 2648–2655.

Takano, T. (1977) *J. Mol. Biol. 110*, 569–584.

Teraoka, J., & Kitagawa, T. (1981) *J. Biol. Chem. 256*, 3969–3977.

Teraoka, J., Job, D., Morita, Y., & Kitagawa, T. (1983) *Biochim. Biophys. Acta 747*, 10–15.

Tien, M. (1987) *CRC Crit. Rev. Microbiol. 15*, 141–168.

Tien, M., & Tu, C.-P. D. (1987) *Nature (London) 326*, 520–523.

Tsubaki, M., Nagai, K., & Kitagawa, T. (1980) *Biochemistry 19*, 379–385.

Valentine, J. S., Sheridan, R. P., Allen, L. C., & Kahan, P. C. (1979) *Proc. Natl. Acad. Sci. U.S.A. 76*, 1009–1013.

Van Wart, H. E., & Zimmer, J. (1985) *J. Biol. Chem. 260*, 8372–8377.

Walters, M. A., & Spiro, T. G. (1982) *Biochemistry 21*, 6989–6995.

Wariishi, H., & Gold, M. H. (1989) *FEBS Lett. 243*, 165–168.
Wariishi, H., & Gold, M. H. (1990) *J. Biol. Chem. 265*, 2070–2077.
Wariishi, H., Marquez, L., Dunford, H. B., & Gold, M. H. (1990) *J. Biol. Chem. 265*, 11137–11142.
Yamazaki, I. (1974) in *Molecular Mechanisms and Oxygen Activation* (Hayaishi, O., Ed.) pp 535–558, Academic Press, New York.
Yamazaki, I., & Piette, L. H. (1963) *Biochim. Biophys. Acta 77*, 47–64.

^{1}H NMR Study of the Influence of Hydrophobic Contacts on Protein–Prosthetic Group Recognition in Bovine and Rat Ferricytochrome b_5†

Kang-Bong Lee, Gerd N. La Mar,* Lisa A. Kehres, Eugene M. Fujinari, and Kevin M. Smith
Department of Chemistry, University of California, Davis, California 95616
Thomas C. Pochapsky‡ and Stephen G. Sligar
Department of Biochemistry and Chemistry, University of Illinois, Urbana, Illinois 61801
Received April 2, 1990; Revised Manuscript Received July 16, 1990

ABSTRACT: The proton nuclear magnetic resonance spectra of the soluble fragment of native bovine and genetically engineered wild-type rat ferricytochrome b_5 reconstituted with a wide variety of hemes chemically modified at 2- and/or 4-positions have been recorded and analyzed. While all but one nonsymmetric heme yielded comparable amounts of the two heme orientations immediately after reconstitution, the relative proportion of the two orientations at equilibrium varied widely. The unpaired spin density distribution in the heme π system leads to substituent hyperfine shift patterns in these paramagnetic complexes that are completely diagnostic of the heme orientation in the protein matrix. An empirical assignment strategy is outlined and applied which allows unequivocal assignment of the absolute orientation of a derivatized heme within the protein matrix. Using a series of hemes lacking 2-fold symmetry solely due to a single substitution, the preferences for localized site occupation of vinyls, methyls, and hydrogens are developed. The large differences in relative stability of the two orientations of native protohemin in the two cytochromes b_5 is shown to result from the additivity of localized effects for the bovine protein and the near cancellation of competing effects in the rat protein. The major determinant of the heme orientation is judged to be a repulsive interaction between a vinyl and a hydrophobic cluster of amino acids including positions 23 and 25. The differences in this heme orientational preference among bovine, rat, and chicken ferricytochromes b_5 could be correlated with the relative steric bulk of the residues at positions 23 and 25. Detailed thermodynamic analysis of the orientational preferences of native protoheme reveals that, while the same orientation as found in X-ray crystal structures of bovine cytochrome b_5 predominate at 25 °C in both proteins, the preference in the bovine protein is primarily for enthalpic reasons while in the rat protein the preference is due to entropic factors.

Cytochrome b_5 is a membrane-bound electron transport protein involved in fatty acid desaturation and the cytochrome P-450 reductase system (Strittmatter et al., 1974). A soluble fragment is found as a component of the hemoglobin reductase system which is essentially identical with the tryptically cleaved microsomal protein (Hultquist et al., 1984). The soluble fragment of the bovine protein has been subjected to the most extensive studies, with details of the protein folding presented in high-resolution X-ray crystal structure of both oxidized and reduced forms (Mathews et al., 1971, 1979; Mathews, 1980). ^{1}H NMR[1] studies have provided information on the solution molecular, electronic, and magnetic properties of the protein that directly demonstrated that the protein in solution is an interconvertible heterogeneous mixture of two isomers (ratio ~ 9:1) that differ by a 180° rotation of the heme about the α,γ-meso axis, as illustrated in parts A and B of Figure 1 (Keller & Wüthrich, 1980; La Mar et al., 1981; McLachlan et al., 1986a,b). The dominant isomer in solution (Figure 1A) is the only one detected in the crystal. The two isomeric forms detectably differ in redox potential as a result of the altered peripheral interaction with the protein matrix (Walker et al., 1988). Preliminary solution ^{1}H NMR spectra of the bacterially expressed soluble fragments of rat microsomal cytochrome b_5 indicated very similar spectral parameters, including two components, but with much more similar relative stability at equilibrium (Rogers et al., 1986).

We are interested in delineating both the factors that control the heme orientational preference in the native bovine protein and the structural basis for the significantly altered preference in the rat versus bovine proteins. Preliminary ^{1}H NMR studies with a limited number of synthetic hemins with modified substituents at the 2- and 4-positions (Figures 1A,B), reconstituted into rabbit cytochrome b_5 with NMR properties in-

†This research was supported by grants from the National Science Foundation, DMB-87-03611, and National Institutes of Health, HL-22252 and GM-33775.
*Address correspondence to this author.
‡Present address: Department of Chemistry, Brandeis University, Waltham, MA 02254.

[1] Abbreviations: NMR, nuclear magnetic resonance; DSS, 2,2-dimethyl-2-silapentane-5-sulfonate; NOE, nuclear Overhauser effect; ppm, parts per million.

0006-2960/90/0429-9623$02.50/0